

Pressure Dependence of the Structure and Properties of Liquid *n*-Butane¹

William L. Jorgensen²

Contribution from the Department of Chemistry, Purdue University, West Lafayette, Indiana 47907. Received February 2, 1981

Abstract: The effects of pressure on the structure, thermodynamic properties, and conformational equilibrium for liquid *n*-butane have been studied via statistical mechanics simulations at 1, 5000, and 15 000 atm. Consistent with Raman experiments on lower *n*-alkanes, increased pressure is found to increase the gauche population in liquid *n*-butane; however, the shift amounts to only a 7% change in the populations in going from 1 to 15 000 atm at -0.5 °C. Various computed properties are found to be in very good agreement with experimental values including the density, heat of vaporization, and compressibility for which the discrepancies are 3, 4, and 10%, respectively, at 1 atm. The sharpening of the radial distribution functions reflects increased structure at higher pressure, though the effects are not striking in stereoplots even at 15 000 atm. Interestingly, the energy of liquid *n*-butane is computed to be lowest at 5000 atm which is in accord with Bridgman's observations in 1913 for a variety of organic liquids. Overall, a key finding is that the simple Lennard-Jones description of the intermolecular interactions remains successful over the pressure range studied which represents a compression of 33%.

I. Introduction

The conformational characteristics of liquid *n*-alkanes and polyethylene at high pressure and the search for ordered phases are under active investigation. The Raman results of Schoen et al. are particularly fascinating; they have found that the lower alkanes under ca. C_{20} show increased folding as pressure is increased from 0 to 20 kbar, while liquid *n*- $C_{40}H_{82}$ reveals the opposite behavior, chain straightening, and the occurrence of an ordered liquid phase, possibly liquid crystalline, before freezing at high pressures.^{3,4} Similar findings have been reported for polyethylene in which case thermodynamic, spectroscopic, and diffraction data indicate an ordered liquid phase before crystallization at around 5 kbar.⁵ In the resultant solid the polyethylene chains are fully extended in contrast to the folded, lamellar morphology that is well known at low pressures.⁶

Monte Carlo statistical mechanics simulations of liquids in the isothermal, isobaric (NPT) ensemble can be used in principle to directly study such problems at the molecular level. In fact, few computations have been performed in this ensemble, though its correspondence with the usual experimental conditions is an obvious advantage over the more common Monte Carlo simulations in the canonical (NVT) ensemble and molecular dynamics calculations which normally take place in the microcanonical (NVE) ensemble. It appears that there have only been three NPT simulations involving molecular liquids reported to date: Owicki and Scheraga's studies of water and a dilute solution of methane in water and Jorgensen and Ibrahim's computations for dimethyl ether.^{7,8} Furthermore, only one pressure, 1 atm, was treated in these works.

In order to further test the capabilities of the theoretical method and to study the structure and conformational properties of a prototype liquid *n*-alkane at high pressures, a series of Monte Carlo simulations for liquid *n*-butane have been carried out in the NPT ensemble as described here. The calculations were all performed

at -0.5 °C, the normal boiling point, and at pressures of 1, 5000, and 15 000 atm. Consistent with the Raman data for the lower alkanes, the gauche population is found to increase with increasing pressure, though the quantitative effects are modest. Some increase in order at higher pressure is witnessed by sharpening of the radial distribution functions; however, even at 15 000 atm liquid *n*-butane is still disordered. A variety of thermodynamic properties including densities, compressibilities, and heats of vaporization have been computed and are in excellent agreement with experimental values. Further insights into the liquid's character at the molecular level are obtained from energy distributions and stereoplots. The discussion also includes comparisons with related experimental results of P. W. Bridgman from the early 1900's. To begin, the computational methodology and conditions are summarized.

II. Liquid Simulations in the NPT Ensemble

Complete presentations of the computational formalism for Monte Carlo simulations in the NPT ensemble can be found in the papers by Owicki and Scheraga⁷ and McDonald.⁹ A key point is that the average value of a property Q for a system of N particles may be represented by eq 1 where Q_k is the kinetic energy con-

$$\langle Q \rangle = Q_k + \int \int Q(X,V)P(X,V) dXdV \quad (1)$$

$$P(X,V) = \exp(-\beta H(X,V)) / \int \int \exp(-\beta H(X,V)) dXdV$$

$$H(X,V) = E(X) + PV(X) \quad \beta = (k_B T)^{-1}$$

tribution and the second term is the configurational integral over all possible geometric configurations, X , and volumes for the system. $P(X,V)$ is the appropriate Boltzmann factor giving the probability of occurrence of the configuration X with volume V , while H is the enthalpy and E is the energy which includes intermolecular and intramolecular terms. In addition to obtaining the energy, enthalpy, and volume from averages like eq 1, other thermodynamic properties, particularly the heat capacity (C_p), isothermal compressibility (κ), and coefficient of thermal expansion (α) can be represented as fluctuations in the former quantities (eq 2-4). Numerous distribution functions describing the

$$C_p = (\partial \langle H \rangle / \partial T)_P = (\langle H^2 \rangle - \langle H \rangle^2) / NkT^2 \quad (2)$$

$$\kappa = -(\partial \langle V \rangle / \partial P)_T / \langle V \rangle = (\langle V^2 \rangle - \langle V \rangle^2) / kT \langle V \rangle \quad (3)$$

$$\alpha = (\partial \langle V \rangle / \partial T)_P / \langle V \rangle = (\langle VH \rangle - \langle V \rangle \langle H \rangle) / kT^2 \langle V \rangle \quad (4)$$

structure and energetics of liquids can also be formulated as configurational averages.

(1) Quantum and Statistical Mechanical Studies of Liquids 19.
 (2) Camille and Henry Dreyfus Foundation Teacher-Scholar, 1978-1983. Alfred P. Sloan Foundation Fellow, 1979-1981.
 (3) Schoen, P. E.; Priest, R. G.; Sheridan, J. P.; Schnur, J. M. *J. Chem. Phys.* **1979**, *71*, 317. Schoen, P. E.; Priest, R. G.; Sheridan, J. P.; Schnur, J. M. *Nature (London)* **1977**, *270*, 412.
 (4) Wunder, S. L.; Cavatorta, F.; Priest, R. G.; Schoen, P. E.; Sheridan, J. P.; Schnur, J. M. *Polym. Prepr., Am. Chem. Soc., Div. Polym. Chem.* **1979**, *20*, 770. Wunder, S. L.; Schoen, P. E.; Schnur, J. M., submitted for publication.
 (5) Tanaka, H.; Takemura, T. *Polym. J.* **1980**, *12*, 349. Wunderlich, B.; Arakawa, T. *J. Polym. Sci., Part A* **1964**, *2*, 3697. Geil, P. H.; Anderson, F. R.; Wunderlich, B.; Arakawa, T. *Ibid.* **1964**, *2*, 3707.
 (6) For a review, see: Keller, A. *Discuss. Faraday Soc.* **1979**, *68*, 145.
 (7) Owicki, J. C.; Scheraga, H. A. *J. Am. Chem. Soc.* **1977**, *99*, 7403, 7413.
 (8) Jorgensen, W. L.; Ibrahim, M. *J. Am. Chem. Soc.* **1981**, *103*, 3976.

(9) McDonald, I. R. *Mol. Phys.* **1972**, *23*, 41.

The configurational integrals are convertible to sums over finite numbers of discrete configurations for computational purposes. However, for the sums to converge at a reasonable rate it is necessary to treat explicitly a relatively small number of molecules and to avoid excessive sampling of high enthalpy configurations with small Boltzmann factors. This problem is handled by using the Metropolis method.¹⁰ First, periodic boundary conditions are employed which means that the liquid is represented by surrounding a central cell containing 50–1000 molecules with images of itself. The cell is usually taken as a cube though other shapes may be used. New configurations are generated by randomly moving a molecule. If the move molecule passes through a cell wall, then an image of it reenters the central cell through the opposite face. In NPT simulations the volume is also periodically changed by scaling the intermolecular separations of all N molecules. For atomic liquids this may be facilitated by using fractional cell coordinates;⁹ however, for molecular systems we prefer using the Cartesian molecular coordinates throughout.

The next key idea to speed convergence in the Metropolis procedure is to select the configurations so that they occur with a probability equal to their Boltzmann factors. This simplifies the averages to eq 5 where M is the total number of configurations

$$\langle Q \rangle = Q_k + \frac{1}{M} \sum_i^M Q(X_i, V_i) \quad (5)$$

sampled. M should be large enough so increasing it does not alter the averages. The properly distributed chain of configurations is then obtained by considering the enthalpy change in proceeding from configuration i to $j = i + 1$. If $H_j \leq H_i$, then H_j is accepted as the new configuration. Otherwise, j is accepted with a probability $\pi_j = \exp(-\beta(H_j - H_i))$. This is implemented by comparing π_j to a random number, x , in the range (0, 1). If $\pi_j > x$, then X_j is accepted; otherwise X_j is taken as identical with X_i and the next move is attempted.

In view of the sampling procedure it is clearly essential to know the energy of a configuration. In the present case this consists of an intermolecular term given by the pairwise sum over all dimerization energies (ϵ_{mn}) within a set cutoff radius of each monomer and an intramolecular term for the internal rotational energy ($V(\phi)$) of the monomers (eq 6). Intramolecular vibrations

$$E(X_i) = \sum_{m < n}^N \epsilon_{mn} + \sum_m^N V(\phi_m) \quad (6)$$

are not considered as the bond lengths and angles in the monomers are fixed. This representation of the energetics was found to be successful in NVT Monte Carlo simulations of liquid methanol,¹¹ ethanol,¹² n -butane,¹³ and 1,2-dichloroethane¹³ which included internal rotation. Fixman showed that adjustments can be made to the rotational potentials to correct for the rigid constraints and that the modifications only amounted to "a few tenths $k_B T$ " for polymer chains.¹⁴ Generally, rotational potentials are not known experimentally to this level of accuracy. In any event, including the Fixman terms in molecular dynamics simulations of n -butane in a Lennard-Jones solvent was found by Chandler and Berne to not affect the computed gauche and trans populations.^{15a} Conformational transition rates, which are not considered here, are more sensitive to the effects.¹⁵

III. Potential Functions and Computational Details

The transferable intermolecular potential functions (TIPS) previously reported for alkanes were used in this work. Each n -butane monomer consists of four interaction sites centered on the carbons, and the hydrogens are implicit. Standard bond

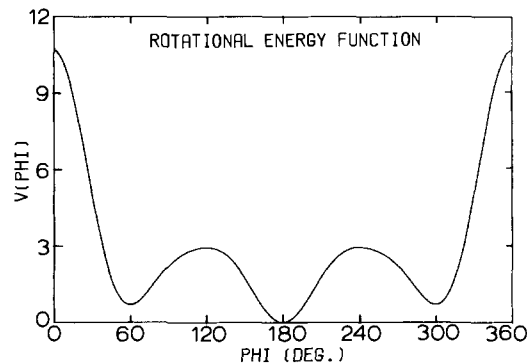


Figure 1. Potential function (kcal/mol) for rotation about the central CC bond in n -butane.

lengths (1.53 Å) and bond angles (109.47°) were assumed. The sites interact intermolecularly via Lennard-Jones terms (eq 7).

$$\epsilon_{mn} = \sum_i^{\text{on } m} \sum_j^{\text{on } n} \left(\frac{A_i A_j}{r_{ij}^{12}} - \frac{C_i C_j}{r_{ij}^6} \right) \quad (7)$$

As in the previous works,^{8,11–13} A^2 values for methyl and methylene groups are 7.95×10^6 and 7.29×10^6 kcal·Å¹²/mol, and the corresponding C^2 parameters are 2400 and 1825 kcal·Å⁶/mol.

The intramolecular rotational potential used here is the revised Scott-Scheraga potential given by eq 8 and illustrated in Figure

$$V(\phi) = 2.218 - 2.905 \cos \phi - 3.136 \cos^2 \phi + 0.731 \cos^3 \phi + 6.272 \cos^4 \phi + 7.527 \cos^5 \phi \quad (8)$$

1. This function was also adopted in the NVT simulation of liquid n -butane.¹³ The potential has trans and gauche minima at dihedral angles of 180° and ±60° with gauche 0.70 kcal/mol above trans and a trans to gauche barrier of 2.95 kcal/mol.

The NPT simulation at 1 atm provides an important test of the potential functions: to see whether they can yield a density for the liquid and other thermodynamic properties in reasonable accord with experiment. The results at higher pressures are an important probe of the range of validity for the potentials. A priori it seems reasonable to expect the Lennard-Jones parameters to be dependent on pressure; some contraction of the atomic radii with increasing pressure might be anticipated (vide infra).

The Monte Carlo calculations were executed using cubic samples of 128 monomers, periodic boundary conditions, and Metropolis sampling. The simulations were run at -0.5 °C, the normal boiling point, and at pressure of 1, 5000, and 15 000 atm. Spherical cutoffs at 12 Å were used in evaluating the dimerization energies which include interactions with a molecule's ca. 50–70 nearest neighbors. New configurations were created by randomly selecting a monomer, translating it in all three Cartesian directions, rotating it about one random axis, and performing the internal rotation. The volume changes were attempted on every 400th move. The ranges for the motions were chosen to yield acceptance rates of 40–50% for new configurations. For the simulations at 1, 5K, and 15K atm the ranges were for the translations (±0.15, ±0.12, and ±0.09 Å), for the total rotations (±15, ±12, and ±9°), for the internal rotations (±15, ±15, and ±12°), and for the volume moves (±600, ±300, and ±175 Å³). Clearly, the increased density at higher pressure required the ranges to be smaller for the acceptance rate to be maintained.

The calculation at 1 atm was initiated from a configuration in the previous NVT simulation.¹³ The higher pressures were achieved in increments of several thousand atmospheres. Equilibration for each run involved 800K–1200K configurations which were discarded. Final averaging took place over an additional 1200K configurations for the simulation at 1 atm and 1500K for the calculations at 5K and 15K atm. Each complete run required 6–7 h on a CDC/7600. Convergence was established by monitoring the inter- and intramolecular energies, conformer populations, and volume. No significant drift in the averages of these quantities occurred during the averaging. The trans-gauche

(10) Metropolis, N.; Rosenbluth, A. W.; Rosenbluth, M. N.; Teller, A. H.; Teller, E. *J. Chem. Phys.* **1953**, *21*, 1087.

(11) Jorgensen, W. L. *J. Am. Chem. Soc.* **1981**, *103*, 341.

(12) Jorgensen, W. L. *J. Am. Chem. Soc.* **1981**, *103*, 345.

(13) Jorgensen, W. L. *J. Am. Chem. Soc.* **1981**, *103*, 677. Jorgensen, W. L.; Binning, R. C.; Bigot, B. *Ibid.* **1981**, *103*, 4393.

(14) Fixman, M. *J. Chem. Phys.* **1978**, *69*, 1527.

(15) (a) Chandler, D.; Berne, B. J. *J. Chem. Phys.* **1979**, *71*, 5386. (b) Pear, M. R.; Weiner, J. H. *Ibid.* **1979**, *71*, 212. (c) Helfand, E. *Ibid.* **1979**, *71*, 5000.

Table I. Thermodynamic Results for Liquid *n*-Butane at -0.5°C

property	pressure		
	1 atm	5000 atm	15 000 atm
$V, \text{\AA}^3$	156.2 ± 0.8	122.8 ± 0.2	107.7 ± 0.1
V (exptl)	160.3^a	$(123)^b$	$(107)^b$
$E^{\text{inter}}, \text{kcal/mol}$	-5.105 ± 0.034	-6.011 ± 0.019	-5.359 ± 0.035
$E^{\text{intra}}, \text{kcal/mol}$	0.561 ± 0.009	0.564 ± 0.011	0.610 ± 0.010
% trans	67.8 ± 1.3	66.4 ± 1.9	61.7 ± 0.9
$\kappa, \text{atm}^{-1} \times 10^{-6}$	148 ± 29	21 ± 3	9 ± 1
κ (exptl)	$(165)^b$	$(18)^b$	$(6)^b$
$\alpha, \text{deg}^{-1} \times 10^{-5}$	115 ± 31	38 ± 10	33 ± 11
α (exptl)	176^a	$(48)^b$	
$C_p^{\text{inter}}, \text{cal/mol-deg}$	8.2 ± 1.4	8.0 ± 1.6	14.5 ± 4.3
C_p	30.0	29.8	36.3
C_p (exptl)	31.8^a		
$\Delta H_V, \text{kcal/mol}$	5.57		
ΔH_V , (exptl)	5.35^a		

^a Reference 16. ^b Estimated, see text.

barrier crossings were also counted during the averaging. For the run at 1 atm there were 523 trans to gauche and 536 gauche to trans crossings. The corresponding figures at 5K atm were 446 and 457, and at 15K there were 389 and 392 crossings. The near equality of these pairs of numbers is also consistent with the equilibration being complete. The conformer populations oscillate in ranges of 4–8% over increments of 100K configurations. Both the 1-atm and 5K-atm were at points of relatively high trans population at the end of the computations which is consistent with the excess of gauche to trans crossings. It should be noted that several crossings are typically needed before a true transition occurs such that the monomer stays in and explores another conformational potential well. Also, no gauche to gauche transitions were observed owing to the higher barrier height and the temperature.

IV. Results and Discussion

(a) **Thermodynamics.** The thermodynamic results from the simulations and the related experimental data are summarized in Table I. The computed standard deviations as shown ($\pm 2\sigma$) were obtained from separate averages over each increment of 100K configurations.

First, the computed molecular volume at 1 atm (156\AA^3) is within 3% of the experimental value which is obtained readily from the density, 0.602 g cm^{-3} .¹⁶ Experimental data on the compressibility of liquid *n*-butane do not appear to be available. However, there is a wealth of data on other *n*-alkanes including *n*-pentane through *n*-decane and it fits simple patterns. The pioneering work in this area is by Bridgman¹⁷ whose results from the first half of the century are in good accord with more recent measurements by Eduljee,¹⁸ Blinowski,¹⁹ and co-workers. The volume changes with pressure for the lower alkanes are similar and the small differences are regular. For example, the volumes of liquid *n*-pentane, *n*-hexane, and *n*-heptane at 0°C and 5000 kg cm^{-2} (4845 atm) are 0.781, 0.807, and 0.815 relative to their volumes at 1 atm being taken as 1.000.¹⁷ Analysis of the large amount of available data^{17–19} leads us to estimate the following relative volumes for liquid *n*-butane at 0°C : 1 atm (1.00), 1000 atm (0.89), 5000 atm (0.77), 10 000 atm (0.71), and 15 000 atm (0.67). The uncertainties in these values are anticipated to be no more than $\pm 3\%$. One might also wonder what the freezing pressure would be for *n*-butane. Again by analyzing the available data for freezing of the lower *n*-alkanes,¹⁷ *n*-butane is expected to require a pressure of $25\,000 \pm 5000$ atm to crystallize at 0°C .

(16) (a) Rossini, F. D.; Pitzer, K. S.; Arnett, R. L.; Brown, R. M.; Pimentel, G. C. "Selected Values of Physical and Thermodynamic Properties of Hydrocarbons and Related Compounds", American Petroleum Institute, Carnegie Press: Pittsburgh, 1953. (b) Aston, J. G.; Messerly, G. H. *J. Am. Chem. Soc.* **1940**, *62*, 1917.

(17) Bridgman, P. W. *Proc. Am. Acad. Arts Sci.* **1931**, *66*, 185; *ibid.* **1949**, *77*, 129.

(18) Eduljee, H. E.; Newitt, D. M.; Weale, K. E. *J. Chem. Soc.* **1951**, 3086.

(19) Blinowski, A.; Brostow, W. *J. Chem. Thermodyn.* **1975**, *7*, 787.

Consequently, the simulations reported here are well below the freezing point.

The computed molecular volumes at 5K and 15K atm are in perfect agreement with the experimental estimates as recorded in Table I. Thus, the potential functions are correctly describing the pressure dependence of the density over the 15K-atm range, which represents a compression of 33%. This is a most remarkable result which supports the viability of the TIPS potentials and the ability to perform meaningful NPT simulations at high pressures. It is emphasized that the same Lennard-Jones parameters, rotational potential, and monomer geometry have been used throughout.

Several other thermodynamic results can also be compared with experimental data. The heat of vaporization was calculated as usual: $\Delta H_V = -E^{\text{inter}}(\text{l}) + E^{\text{intra}}(\text{g}) - E^{\text{intra}}(\text{l}) - (H^\circ(\text{g}) - H(\text{g})) + P(V(\text{g}) - V(\text{l}))$.¹³ The intermolecular energies, E^{inter} , reported in Table I include cutoff corrections¹³ which amount to -0.26 , -0.33 , and -0.38 kcal/mol for the simulations at 1, 5K, and 15K atm, respectively, and the enthalpy departure function for the real gas ($H^\circ - H$) is 0.08 kcal/mol at -0.5°C and 1 atm.¹³ The net result is a computed ΔH_V at 1 atm of 5.57 kcal/mol which is only 4% higher than the experimental value, 5.35 kcal/mol.^{16b}

The contribution to the heat capacity from the intermolecular energy, C_p^{inter} , can be added to the unimolecular term approximated by the heat capacity of the ideal gas, C_p° , to calculate the total C_p . The computed C_p 's are relatively constant, though some increase is observed at 15K atm. This behavior is in agreement with Bridgman's results for a variety of organic liquids at ca. 1–12K atm in his classic paper of 1913.²⁰ His study did not include pure hydrocarbons; however, alcohols, diethyl ether, acetone, and alkyl halides all exhibit small effects of pressure on C_p . There is a slight decrease in C_p from 1 to about 2000 atm followed by a gradual increase in C_p at higher pressures.²⁰ It is also noted that the computed C_p at 1 atm is in very good agreement with the experimental value (Table I), though it should be realized that the ideal gas term accounts for 73% of the total. Furthermore, the fluctuation properties given by eq 2–4 are well known to converge relatively slowly and have substantial error bars as shown in Table I.

The isothermal compressibilities, κ , have been reported for many *n*-alkanes except *n*-butane but again are quite regular. The dependence of a liquid's volume on pressure is generally well described by the Tait equation (eq 9) where B and C are constants

$$\Delta V/V_0 = C \log[(B + P)/(B + P_0)] \quad (9)$$

for each system with C relatively invariant at ca. 0.22 for *n*-alkanes.¹⁸ Given this relation, then $\kappa = C/[2.303(B + P)]$ which shows κ decreases as $1/P$. At 0°C and 1 atm the κ 's for *n*-hexane, *n*-heptane, and *n*-octane are 132×10^{-6} , 119×10^{-6} , and $101 \times 10^{-6} \text{ atm}^{-1}$ from Eduljee's data.¹⁸ Further application of the Tait relationships then yields essentially constant values of 17×10^{-6} and $6 \times 10^{-6} \text{ atm}^{-1}$ for the three liquids at 5K and 15K atm and 0°C . The values are independent of the liquid owing to the dominance of P over B at high pressure in the expression for κ . Based on these results and additional data of Blinowski and Brostow,¹⁹ κ 's for liquid *n*-butane may be predicted to be 165×10^{-6} , 18×10^{-6} , and $6 \times 10^{-6} \text{ atm}^{-1}$ for pressures of 1, 5K, and 15K atm. The computed values in Table I are in very good accord with these estimates in view of the statistical and experimental uncertainties.

The coefficient of expansivity, α , is available at 1 atm and 0°C from density data for *n*-butane.^{16a} The experimental value of $176 \times 10^{-5} \text{ deg}^{-1}$ is higher than the computed value of $(115 \pm 31) \times 10^{-5} \text{ deg}^{-1}$ obtained from eq 4. Some of the discrepancy is due to the fact that the computed α should be corrected for a unimolecular contribution from the neglected vibrations as for C_p . A value at 5000 atm can also be estimated from Bridgman's and Eduljee's data for *n*-pentane through *n*-heptane. The α for these three liquids at 5000 atm and 0°C is essentially constant at $(45 \pm 2) \times 10^{-5} \text{ deg}^{-1}$ which is again somewhat greater than

(20) Bridgman, P. W. *Proc. Am. Acad. Arts Sci.* **1913**, *49*, 3.

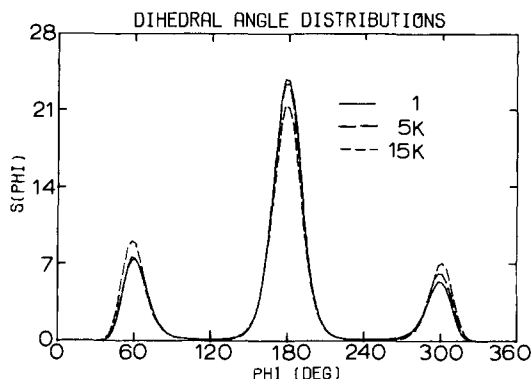


Figure 2. Computed population distributions for the dihedral angle about the central CC bond in *n*-butane. Results are shown for the liquid simulations at 1, 5K, and 15K atm.

the computed value for *n*-butane in Table I. Insufficient experimental data are available to estimate α at 15K atm.

(b) Internal Rotation. The computed distributions for the dihedral angle, $s(\phi)$, in the monomers are illustrated in Figure 2. In agreement with the Raman results for the lower *n*-alkanes,³ the gauche population is found to increase with increasing pressure. This prediction was also made earlier by Pratt et al. on the basis of RISM calculations.²¹ Qualitatively, the effect may be attributed to the gauche monomers having a smaller molecular volume owing to mutual shielding of the methyl groups. However, the quantitative shifts found here are quite small. Specifically, the trans populations are obtained by integrating $s(\phi)$ from 120 to 240° with the remaining monomers being gauche. The results in Table I reveal a decline in the trans population of 7% in going from 1 to 15K atm. It is difficult to compare this with the shifts in the Raman spectra because of the differences in the liquids and uncertainties in relating the Raman intensities to conformer populations at different pressures. Nevertheless, the changes in the Raman spectra for *n*-hexane and *n*-heptane are modest up to about 8K atm.³ It may also be noted that Pratt et al. estimated a ΔV of $-2 \text{ cm}^3/\text{mol}$ for the trans-gauche equilibrium in *n*-butane.²¹ Using this value and the relationship, $\ln(K_2/K_1) = -\Delta V(P_2 - P_1)/RT$, predicts the trans population to decrease by ca. 30% in going from 1 to 15K atm, though ΔV may not be independent of pressure. Based on the results reported here a less negative estimate for ΔV of about $-0.4 \text{ cm}^3/\text{mol}$ can be made.

A few comments on convergence are again in order. The asymmetry in Figure 2 shows that during the averaging there were slight excesses of gauche⁻ molecules over gauche⁺. The largest difference is at 15K atm where the gauche⁻ and gauche⁺ populations are 21.9 and 16.4%, respectively. This means that on the average there were 28 gauche⁻ and 21 gauche⁺ molecules. The original configuration had an excess of about 4 gauche⁻ molecules. As discussed previously,¹³ with small sample sizes and reasonable length runs it would be fortuitous for these numbers to exactly balance. In any event, there is strong evidence to support the convergence of the overall trans and gauche populations. A key test was made in the NVT work in which two simulations were run starting with the monomers all cis in one and all trans in the other.¹³ The energies and populations converged to the same values within 800K configurations. Owing to the more reasonable starting configurations convergence was more rapid for the NPT runs. In both the NPT and NVT simulations no drift in the averages for the energies and populations was observed after equilibration.

Finally, it is noted that the NVT results at the normal liquid density and the NPT results at 1 atm are essentially identical since the error in the computed density was small. Thus, the computed trans populations at $-0.5 \text{ }^\circ\text{C}$ are (67.1 ± 0.8) and $(67.8 \pm 1.3)\%$ from the NVT and NPT calculations, respectively. Both numbers are the same as the trans population for the ideal gas (67.7%) obtained from a Boltzmann distribution for eq 8 at $-0.5 \text{ }^\circ\text{C}$.

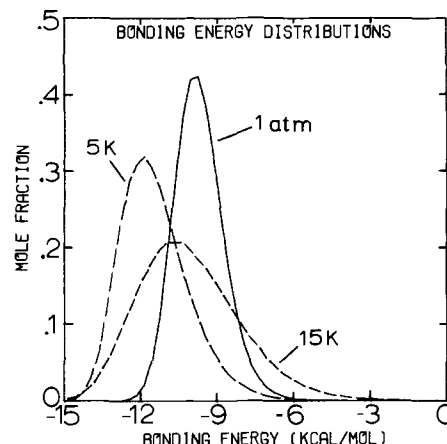


Figure 3. Computed distributions of intermolecular bonding energies for monomers in liquid *n*-butane at the three pressures. The units for the ordinate are mole fraction per kcal/mol.

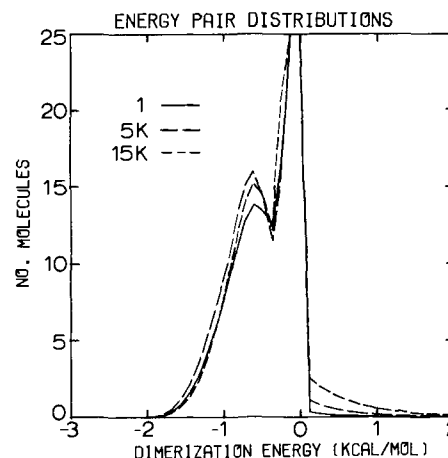


Figure 4. Computed distributions of dimerization energies for a monomer in liquid *n*-butane at the three pressures. The units for the ordinate are molecules per kcal/mol.

Consequently, there is no condensed-phase effect on the conformational equilibrium for liquid *n*-butane at 1 atm and the effects are modest even to 15K atm.

(c) Energy Distributions. The distributions for the total intermolecular bonding energies for monomers in liquid *n*-butane are shown in Figure 3. Unimodal distributions that broaden with increasing pressure are found. The pressure effects are substantial in this case. Interestingly, as shown in the figure and by the E^{inter} values in Table I, the intermolecular interactions are most attractive at 5000 atm. Bridgman also studied this problem and showed in his 1913 paper that the internal energy for many organic liquids reaches a minimum at 4000–9000 atm.²⁰ For *n*-pentane, he observed that $(\partial E/\partial P)_T = 0$ when the relative volume is 0.77 which at $0 \text{ }^\circ\text{C}$ corresponds to a pressure of 5500 atm.¹⁷

The origin of the phenomenon is intimately related to understanding molecular forces and has been addressed by several investigators including Hildebrand²² and Bridgman.^{17,20} Specifically, Bridgman stated: "We should expect, therefore, that at low pressures the internal energy would decrease with rising pressure, the attractive forces being in the ascendant, but at the higher pressures, where the forces resisting compression have become dominant, that the energy would increase with rising pressure."²⁰ It is clear that to a liquid there is nothing special about 1 atm. Further compression leads to more interactions being reached when the repulsive walls begin to be climbed. These notions are consistent with the thermodynamic relation, $(\partial E/\partial V)_T = T(\partial P/\partial T)_V - P$. Both terms on the right-hand side are positive.

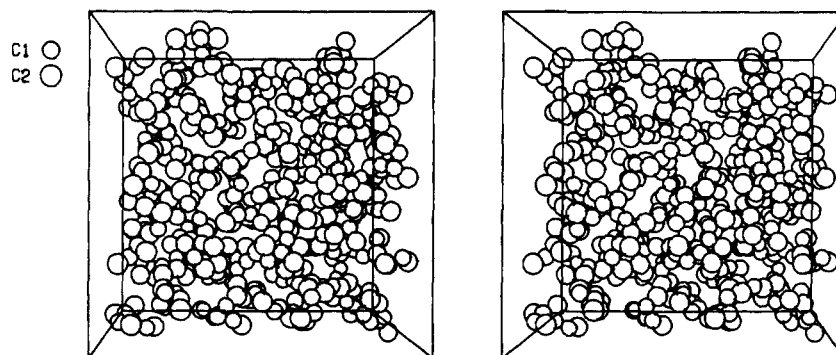


Figure 5. Stereoplot of a configuration from the simulation of liquid *n*-butane at 1 atm. The periodic cube contains 128 monomers.

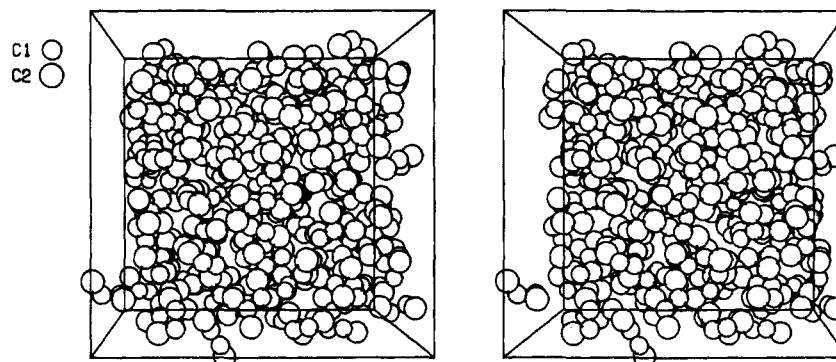


Figure 6. Stereoplot of a configuration from the simulation of liquid *n*-butane at 15K atm. The periodic cube contains 128 monomers.

At low P the first term dominates and $(\partial E/\partial V)_T$ is positive so E is lowered by reducing V . At high P the $-P$ term dominates and $(\partial E/\partial V)_T$ becomes negative so E is increased by further compression.

The distributions of dimerization energies that a monomer experiences on the average are shown in Figure 4. The spikes near 0 kcal/mol are due to the weak interactions between the many distant molecules in the bulk and the reference monomer, while the shoulders at low energy represent the particularly constructive interactions with near neighbors. The strongest attractions between two monomers amount to about 2 kcal/mol. This figure is independent of pressure since the same potential functions are used throughout. The results are consistent with the discussion above since the largest number of attractive interactions is found for the 5000-atm run. Integration reveals that the number of neighbors in the low energy shoulders is ca. 10.6, 12.0, and 10.9 for the simulations at 1, 5K, and 15K atm, respectively. It is also apparent from Figure 4 that the number of repulsive dimer interactions increases uniformly with increasing pressure.

(d) Structure. A direct way to study the structure of the liquids is to analyze stereoplots of configurations from the simulations. Examples from the runs at 1 and 15K atm are shown in Figures 5 and 6. In viewing the plots the periodicity should be kept in mind; molecules near one face of the cube are also near molecules on the opposite face. Furthermore, the cube outlined in the drawings is somewhat outside the borders of the periodic cube which is better defined by the outermost midpoints of the central CC bonds in the monomers. One last point is that the radii of the circles representing the alkyl groups in the drawings have been scaled in proportion to the change in the average length of an edge of the periodic cube in going from 1 to 15K atm. The original sizes of the circles at 1 atm were chosen for visual clarity and are not physically significant.

The higher density at 15K atm is obvious in comparing the drawings. The packing is much tighter at the higher pressure, the intermolecular void spaces are substantially reduced, and there are more short intermolecular distances. However, even at 15K atm and -0.5 °C there are no obvious indications of parallel alignment of monomers or replicated packing of neighbors. This seems consistent with the roughly 3:2 mixture of *trans* and *gauche* monomers; enhanced order and packing would presumably favor

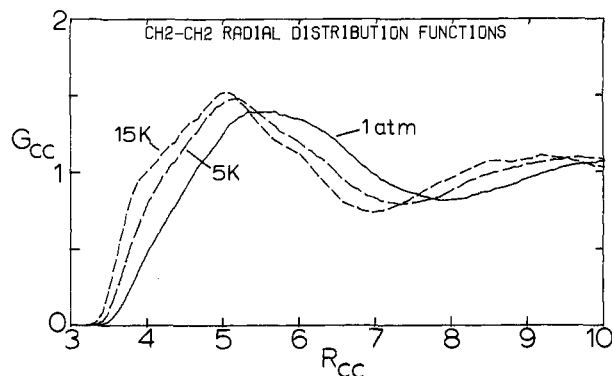


Figure 7. Computed intermolecular $\text{CH}_2\text{-CH}_2$ radial distribution functions for liquid *n*-butane at the three pressures. Distances are in angstroms throughout.

a high *trans* population in view of the crystal structures for *n*-alkanes.²³

The traditional diagnostic for structure in liquids is the radial distribution functions (RDF's), $g_{xy}(r)$, which represent the deviations for distributions of atoms in the liquid from what is given by the bulk density. Specifically, $g_{xy}(r) = \langle N_y(r, r + dr) \rangle / 4\pi\rho_y r^2 dr$ where the numerator is the average number of y atoms around an atom of type x in the shell between r and $r + dr$ and the denominator normalizes g to be unity if N_y is in accord with the bulk density, $\rho_y = (N_y/V)$. Thus, peaks in g_{xy} are associated with shells of neighbors and troughs with the less populated intermediate regions.

The RDF's for the intermolecular interactions in liquid *n*-butane are shown in Figures 7-9 for the $\text{CH}_2\text{-CH}_2$, $\text{CH}_2\text{-CH}_3$ and $\text{CH}_3\text{-CH}_3$ pairs, respectively. As could be expected for an increase in density, the peaks are sharpened and shifted to shorter intermolecular distances with increasing pressure. Therefore, some increase in order accompanies compression. The sharpening of the first peak in the $\text{CH}_3\text{-CH}_3$ RDF is the most pronounced which is reasonable since the methyl groups are the most exposed and

(23) Mathisen, H.; Norman, N.; Pedersen, B. F. *Acta Chem. Scand.* **1967**, *21*, 127. Norman, N.; Mathisen, H. *Ibid.* **1972**, *26*, 3913.

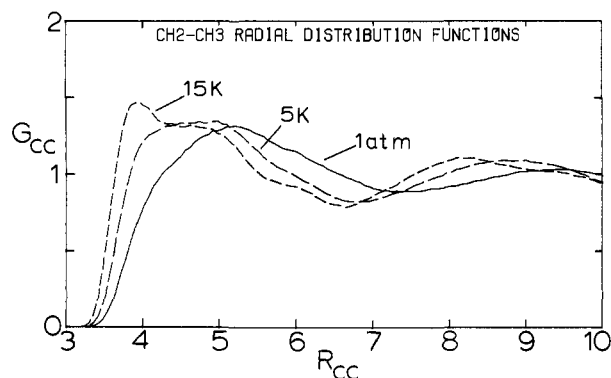


Figure 8. Computed intermolecular $\text{CH}_2\text{-CH}_3$ radial distribution functions for liquid *n*-butane at the three pressures.

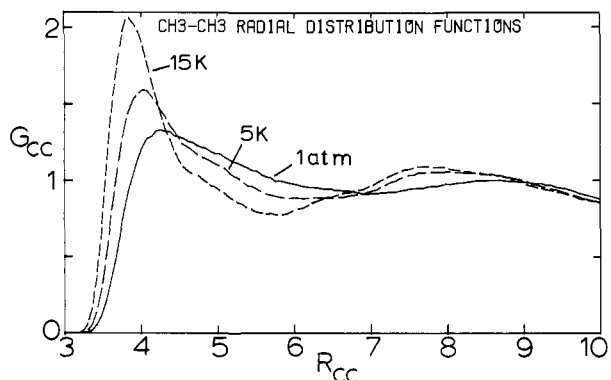


Figure 9. Computed intermolecular $\text{CH}_3\text{-CH}_3$ radial distribution functions for liquid *n*-butane at the three pressures.

consequently critical for efficient packing. Nevertheless, the peaks in the RDF's remain quite broad which is characteristic of non-polar and dipolar aprotic organic liquids.^{8,13} Modest structure is indicated in comparison to hydrogen-bonded liquids such as alcohols and water that have much narrower and sharper first peaks with heights near 3.^{11,12,24}

Estimates for coordination numbers can be obtained by integrating the first peaks in the RDF's. From the $\text{CH}_2\text{-CH}_2$ RDF's, the average number of neighbors for a monomer is 13 at all three pressures. The neighbors are clearly packed more closely at high pressure since the integration limit shifts from 7.9 to 7.4 to 6.9 Å along the series.

Overall, in view of the crystal structures, Raman data, and results presented here, it is reasonable to propose that there are

two competing effects controlling the structure of liquid *n*-alkanes under pressure. A unimolecular term favors increased coiling at higher pressures, while intermolecular interactions and packing prefer extended chains. For the shorter alkanes, the unimolecular effect dominates and for the longer alkanes the intermolecular terms win out. On the basis of the Raman results, the crossover point is in the vicinity of C_{20} .^{3,4} The proposal could be tested by studying the pressure dependence of the Raman spectra for the longer *n*-alkanes in dilute solution with isotropic solvents such as CCl_4 . Under these conditions the unimolecular term should be controlling.

V. Conclusion

It has been demonstrated here that statistical mechanics simulations can be successfully carried out for organic liquids under high constant pressure conditions. Many computed thermodynamic properties, most significantly the density, were found to be in very good agreement with experimental observations or estimates for liquid *n*-butane between 1 and 15 000 atm at -0.5°C . Notably, the simple Lennard-Jones description of the intermolecular interactions remained adequate across this range which corresponds to a 33% compression. Consistent with Raman results for the lower *n*-alkane liquids, *n*-butane has a tendency to coil under pressure showing a 7% increase in the population of gauche monomers in going from 1 to 15 000 atm at -0.5°C . The opposite behavior has been observed for higher *n*-alkanes which may be attributed to intermolecular effects. Another key finding is that the computed radial distribution functions reflect increased order at higher pressure, which is consistent with the concomitant tighter packing clearly apparent in stereoplots.

Although this work supports the feasibility of future theoretical studies of the effects of pressure on organic liquids and solutions, it is important to emphasize that convergence of the calculations must always be carefully considered. This is particularly critical at high pressure because of the more restricted freedom of motion for the monomers at high density. In the present case this necessitated relatively long Monte Carlo runs of 2-3 million configurations each. Properly applied, Monte Carlo simulations in the NPT ensemble provide an exciting opportunity for studying the structures and properties of organic liquids under extreme pressure and temperature conditions.

Acknowledgment. The calculations were carried out on the CDC/7600 system at the Lawrence Berkeley Laboratory under a grant from the National Resource for Computation in Chemistry which was supported by the National Science Foundation (CHE-7721305) and the Basic Energy Science Division of the U.S. Department of Energy (Contract No. W-7405-ENG-48). The author is also grateful to the National Science Foundation (CHE8020466) for aid and to Drs. B. Bigot, J. C. Owicki, and P. E. Schoen for helpful discussions.